Journal of Machine Construction and Maintenance
QUARTERLY ISSN 1232-9312 1/2019(112)
p. 39–46

Sylwia SOWA[a, b, *], Nhu-Tarnawska Hoa KIM-NGAN[b], Magdalena KRUPSKA-KLIMCZAK[b], Volodymyr BUTURLIM[c], Daria DROZDENKO[c], Peter MINARIK[c], Ladislav HAVELA[c]

[a] Institute for Sustainable Technologies – National Research Institute, Radom, Poland
[b] Institute of Physics, Pedagogical University, Cracow, Poland
[c] Faculty of Mathematics and Physics, Charles University, Prague, Czech Republic
* Corresponding author: sylwia.sowa@itee.radom.pl

STABILIZATION OF THE CUBIC γ-U STRUCTURE IN U-T ALLOYS (T = Mo, Pt, Nb, Ru, Ti)

Key words: crystal structure, cubic γ-U phase, X-ray, EBSD.

Abstract: We present the results of the stabilization of the γ-U phase with a cubic structure in U-T alloys by means of combined ultrafast cooling (with a cooling rate 106 K/s) and doping with alloying elements in the VI and VIII group (T = Mo, Pt, Nb, Ru, Ti). The X-ray diffraction data have confirmed the cubic structure presented in all U-T alloys with the alloying element content T≥15 at.% (atomic percentage concentration). Some results of the microstructure analysis, phase distribution and orientation of selected samples by using electron backscatter diffraction are also shown.

STABILIZACJA STRUKTURY KUBICZNEJ γ-U W ZWIĄZKACH U-T (T = Mo, Pt, Nb, Ru, Ti)

Słowa kluczowe: struktura krystaliczna, kubiczna faza γ-U, X- ray, EBSD.

Streszczenie: Zaprezentowaliśmy wyniki stabilizacji fazy γ-U ze strukturą kubiczną w związkach U-T za pomocą techniki ultraszybkiego chłodzenia (z szybkością chłodzenia 106 K/s) oraz domieszkowania pierwiastkami z grup VI i VIII (T= Mo, Pt, Nb, Ru, Ti). Dane dyfrakcji rentgenowskiej potwierdziły obecność kubicznej struktury we wszystkich związkach U-T posiadających zwartość pierwiastków domieszkujących T≥15 at.% (procent atomowy). Wyniki analizy mikrostruktury, rozkładu fazowego i orientacji wybranych próbek zostały również pokazane, używając dyfrakcji wstecznego rozpraszania elektronów.

Introduction

The interest in stabilization of U-based alloys crystallizing in the cubic structure (the so-called γ-U phase) has come from the metallurgy viewpoint. Massive research programs in the USA were launched in the late 1970s (e.g., Reduced Enrichment for Research and Test Reactor (RERTR)) to convert the high-enriched uranium (HEU) fuel to low-enriched uranium fuel (LEU, <20% ^{235} U) [1,2]. The most promising candidates were U-Mo alloys with a Mo concentration of 7–10 wt.%, (weight percentage concentration), since they fulfil the requirements to use as LEU fuel while also preserving the cubic γ-U phase with a higher density and higher stability under irradiation (they are more resistant to swelling than α-U based fuels) [3, 4].

Pure uranium metal exists in three allotropic phases [5]. The orthorhombic α-U phase with space group *Cmcm* is stabilized below 940 K, the tetragonal β-U phase with space group *P42/mmm* exists between 942–1049 K [6], and the γ-U phase with a body centred cubic A2-type structure with space group $Im\bar{3}m$ is stable at high temperatures between 1049–1408 K [7]. The low-temperature properties of uranium have been mostly known for the orthorhombic α-U phase, since only this phase is stable at and below room temperature [6], e.g. it exhibits a superconducting state below the critical temperature T_c = 0.78 K [8–10].

We focused our attention on the stabilization of the γ-U phase by means of combined splat-cooling (with cooling rate 10^6 K/s) and T alloying (T = Mo, Pt, Nb, Ru, Ti). In general, in order to obtain the single

γ-U phase at room temperature, a large concentration of these elements is required to be added in the alloy. Mo has a high solubility in U (≈35at.% (atomic percentage concentration)) and thus is considered as a good candidate for stabilizing the γ-U phase. For instance, the single-phase γ-U alloy has been reported for U-8 wt.% Mo (≈ U-16.5 at.% Mo) under normal furnace conditions [3].

Our earlier results demonstrated that alloying by Mo and Zr in a combination with an ultrafast cooling technique can retain the γ-U phase down to room temperatures with a lower Mo and Zr content [11–13]. In the present work, our results obtained for selected U-T alloys with T = Mo, Nb, Pt, Ru and Ti is summarised. The microstructure analysis (phase distribution and orientation) of selected alloys have also been described.

1. Sample synthesis and experimental details

U-T alloys with various concentrations of alloying element were prepared (T = Mo, Zr, Pt, Nb, Ru, Ti) using natural U (2N8 purity) and T element (4N) by arc melting on a copper crucible in an argon atmosphere in an arc-furnace (Fig. 1a). To obtain good homogenization, the ingots were turned over and remelted 3 times. Up to 4 samples could be obtained in one arc-melting cycle without breaking the vacuum conditions. The mass of each sample is about 200–300 mg, which is suitable for sample preparation by the ultrafast cooling method.

Each sample ingot was loaded into the splat cooling system (high-vacuum splat cooler by Vakuum Praha (Fig. 1b), which provides a cooling rate up to 10^6 K/s. The chamber is pumped to a pressure below $3 \cdot 10^{-5}$ mbar and refilled by argon and them pumped again 3 times. The alloy-ingot was re-melted by an electrical arc in an argon atmosphere. A molten drop of the alloy then falls between the two copper pistons (anvils). A photoelectric switch (activated by the infrared light) would initiate the piston activation so that the falling drop is entrapped between the two piston heads. The resulting sample, the so-called "splat", has a shape of an irregular disc of approx. 20 mm in diameter and 100–200 μm in thickness, as shown in Fig. 2a.

For U-T alloys with T = Mo, Zr, Nb, Ru, Ti we could produce the splats with the wide T-concentration range without any major difficulty, despite fact that we would need to change and choose proper technical parameters (e.g., the anvils power and triggering time). The preparation of splats of the U-Pt and U-Pd alloys turned out to be trickier. The thin splat-cooled disc could be easily formed for the Pt/Pd concentration up to 5 at.% by using standard parameters of the splat-cooler. With increasing Pt/Pd concentration, the variation of melting temperatures and of the surface tension of the melt makes the splat formation progressively difficult. In most cases, the samples of a much higher thickness

a) b)

Fig. 1. The arc furnace (a) and the high-vacuum splat-cooler by Vakuum Praha (b)

a) b)

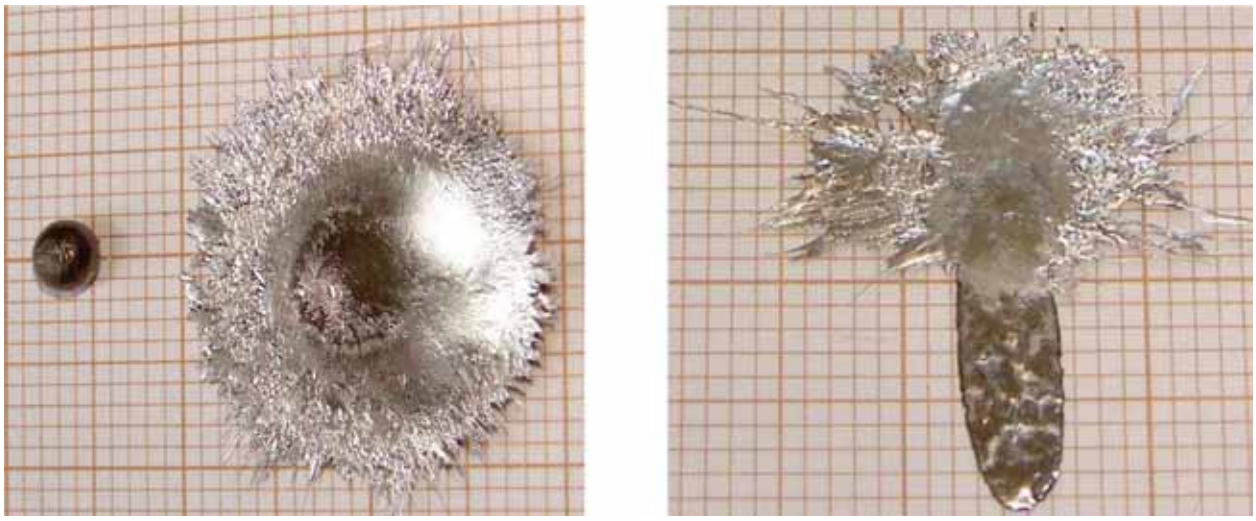

Fig. 2. a) Photograph of the bulk ingot (with a mass of 200–300 mg) prepared by the arc furnace and the resulting splat, a disc with a typical thickness of d = 100–200 μm produced by the splat cooler.b) Photograph of the elongated shape splat (the so-called drop-like splat) with d>250 μm

(d>250 μm) with an elongated shape inherited from the falling drop was obtained, which is shown as an example in Fig. 2b [13,14].

We use sample notations such as $U_{1-x}T_x$ or U-*x* at.% T. For example, the alloy with 15 at.% Ru doped in U are denoted as $U_{0.85}Ru_{0.15}$ and/or U-15 at.% Ru.

The crystal structure investigations were performed using the Brucker D8 Advance (a powder diffractometer with Cu-Kα radiation). The splats are very hard, which cannot be crushed into powders. Besides, we want to avoid any mechanical load on the sample. Thus, it was performed on the whole surface of the splat.

The microstructure analysis of a fraction of splat-cooled alloy was investigated using a Scanning Electron Microscope (SEM) equipped with an energy dispersive X-ray (EDX) analyser. Our splats show a homogeneous distribution of the alloying elements with concentrations corresponding to the nominal ones. Electron backscatter diffraction (EBSD) analysis was employed to study the phase distribution and the orientation of selected U-T splats [11].

2. Results and discussion

2.1. Crystal structure of U-T splats

For an easier comparison of the X-ray data of different U-T alloys, we used normalized ones, in which the intensity of the most intense reflection was normalized to 1. It is then shifted upwards/downwards along the *y*-axis with respect to each other for guiding the eyes. The XRD patterns of U-Mo splats with different Mo concentrations in the range of 0–15 at.% are shown in Fig. 3a. The XRD pattern of a pure U splat (0 at.% Mo) revealed all α-U peaks (e.g., α(021)) and some reflections attributed to γ-U (e.g., the most intense γ(110) one). It was reported earlier that the mixed (α+γ) phase was found in U-Mo alloys with 3.3–6 at.% Mo [14, 15]. In our case, the mixed (α+γ) phase structure was presented in the splat-cooled U-Mo alloys with Mo concentrations ≤10 at.%. For alloys with ≥11 at.% Mo, the X-ray pattern revealed only the γ-type reflections, without any trace of the orthorhombic α-U phase. The alloys with 11–12 at.% Mo showed that they consisted of the tetragonally distorted variant of the cubic γ-U structure (the γ^0-U phase), which is revealed by the splitting of the γ-reflections into doublets. For instance, the γ(110) reflection is split into γ^0(101) and γ^0(110) at angles of 37.0º and 37.2° respectively. In U-12.5at.%Mo, all high-angle γ-reflections are revealed as single peaks. For the prominent γ(110) reflection, however, a small trace of γ(101) reflection was present, which was revealed by a shoulder-like feature of the γ(110) reflection, indicating that a small tetragonal distortion still existed. The XRD pattern indicates that the pure cubic phase was obtained for U-13 at.% Mo and U-15 at.% Mo. However, the observed γ-peaks for U-13 at.% Mo were not as sharp as those for U-15 at.% Mo. The very sharp γ-U peaks in U-15 at.% Mo indicated that this alloy crystalizes in an ideal cubic A2 structure [11].

In the case of the U-Ru system (Fig. 3b), the results showed that U-5 at.% Ru exhibits the mixed orthorhombic and cubic (α'+ γ) phase. (The difference between α' and α orthorhombic structure relates to a relative contraction of the *b* parameter [16, 17]). This (α' + γ) mixture was present in the splats with Ru content up to 10 at.%. Moreover, we found that the lattice parameter *b* was decreased when increasing the Ru concentrations, e.g., *b* = 5.81 Å, *b* = 5.80 Å, *b* = 5.79 Å

was estimated respectively for alloys with 5 at.%, 8 at.% and 10 at.% Ru [18]. Similar to other investigated U-T splats [19, 20], the γ-U phase developed and become dominant with increasing Ru content. Our results indicate that, for a stabilization of the pure cubic γ-U phase, the amount of 12–15 at.% Ru was efficient. Higher Ru concentrations (e.g., 16–18.5 at.%) would lead to an appearance of the U_2Ru compound-the first intermetallic phase in the U-Ru system [18].

More details of magnified X-ray results for U-Ru splats are shown in Fig. 4a. As mentioned above, our results indicated that the pure cubic γ-U structure is stabilized for 12–15 at.% Ru. Namely, the single-type γ-U reflections are revealed for ≥12 at.% Ru. The U_2Ru phase is present for U-16 at.% Ru revealed by an additional signal at 39°. The intensity of this reflection is increased visibly with increasing Ru concentrations from 16 to 18.5 at.% [18].

Figure 4b presents a comparison of the most intense reflection in the X-ray pattern around 37º for U-15 at.% T alloys. As we mentioned earlier, the XRD pattern of U-15 at.% Ru splat is very similar to that of U-15

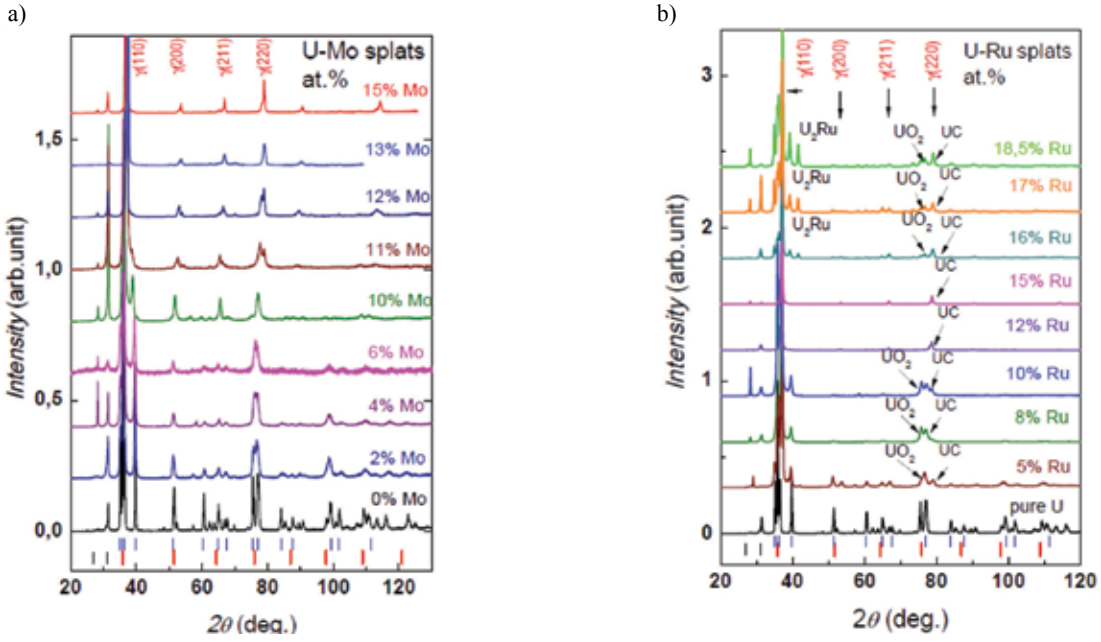

Fig. 3. X-ray diffraction pattern of U-Mo splats (a) and of U-Ru splats (b) for various Mo/Ru concentrations. The colour (vertical) ticks indicate the position of the main reflections of the orthorhombic α-U (blue) and cubic γ-U (red) structures [11, 18]

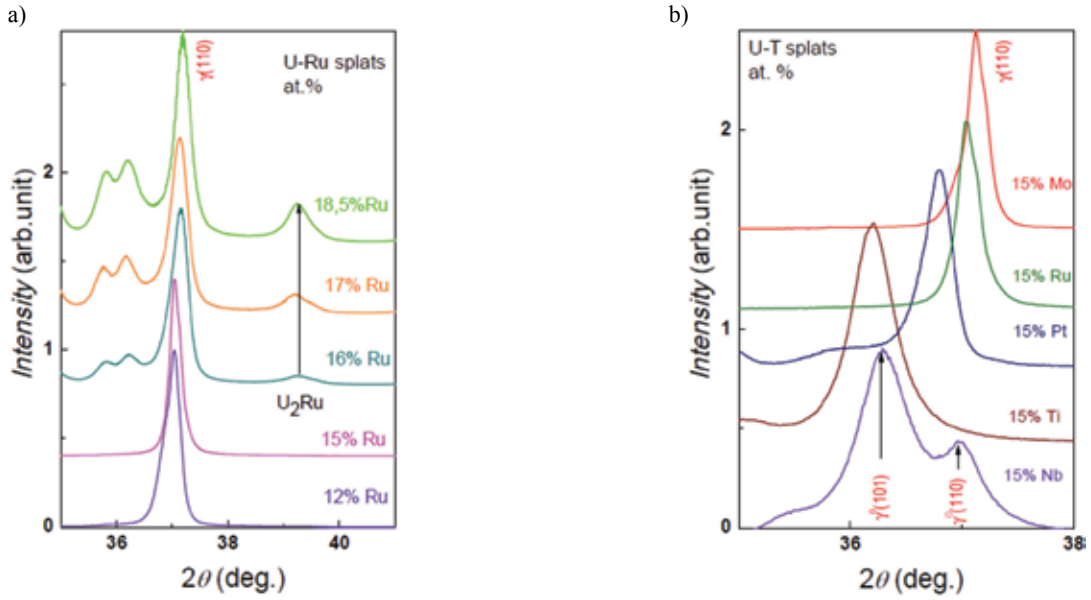

Fig. 4. The magnified XRD pattern of U-T splats: a) A comparison of the most intense reflection in U-Ru system with different Ru content of 12-18.5 at.% Ru; b)A comparison of the γ(110) reflection in the splat with the same T concentration of 15 at.%

at.% Mo splat, exhibiting the pure cubic structure. The cubic γ-U phase could also be stabilized in U-15 at.% Pt, but a small trace of an orthorhombic α-U phase is still present, i.e., a broadening of the γ(110) peak similar to that in U-13 at.% Mo was observed [18]. Moreover, the α(021) peak still existed. It was known that the maximum of Pt and Pd solubility in γ-U was 5 at.%. Our results showed that, by using splat-cooling, we can retain the cubic structure to low temperatures and extend its occurrence for much higher Pt concentrations, at least to 15 at.% [19, 20]. In the case of the U-Ti system, a mixture of the (α +γ) phase was present up to 15 at.% Ti. (The pure γ-U structure was obtained for U-30 at.% Ti). Alloying with 15 at.% Nb seems to stabilize the tetragonally distorted γ°-U phase, which is revealed by the splitting of γ-reflections into doublets (which is similar to U-11/12 at.% Mo). The only difference is that *c/a* ratio of about 0.98–0.99 is estimated for U-Mo alloys, while it amounts to 1.04 for the U-Nb system attributed to a small contraction (in U-Mo) and/or the expansion (in U-Nb) of the *c*-axis of the cubic cell. (The pure γ-U phase was obtained for U-20 at.% Nb) [11, 21]. The lattice parameters estimated for the U-T alloys are given in Table 1.

Table 1. Lattice parameters of selected U-T splat:. α denotes the orthorhombic structure, α' denotes the orthorhombic one with a contraction of the b parameter, γ° denotes the tetragonally distorted γ-U structure (a/c = 0.98–1.04) and γ denotes the cubic γ-U structure (a = c)

T concentration	Structure type	*a,c* (Å)
Pure U	α	
11 at.% Mo	γ°	3.484(a), 3.404 (c)
12 at.% Mo	γ°	3.445(a), 3.396(c)
15 at.% Mo	γ	3.441
15 at.% Nb	γ°	3.434(a),3.565(c)
20 at.% Nb	γ	3.445
15 at.% Pt	γ(+α)	3.469
12 at.% Ru	γ	3.442
15 at.% Ru	γ	3.431
16 at.% Ru	γ (±U_2Ru+α')	3.421
17 at.% Ru	γ (±U_2Ru+α')	3.420
18.5 at.% Ru	γ (±U_2Ru+α')	3.415
15 at.% Ti	γ(+α)	3.510
30 at.% Ti	γ	3.431

2.2. Microstructure of selected U-T splats

All investigated samples were first mechanically polished on SiC grinding papers to study the microstructure. The second step of preparation was Ar ion milling in the Precision Ion Polishing System (PIPS) to remove the surface oxide. It is difficult to get an oxidized-free surface for U-T splats which could diffract. The best EBSD maps were obtained for the pure U splat and for the U-15 at.% Mo splat [14].

EBSD maps recorded the crystallographic orientation and phase distribution from the pure uranium splat surface, which are presented in Fig. 5. It indicates a dominant α-U structure (green colour) with rare, isolated grains of γ-U typically no more than 1 μm in maximum dimension [11]. The grain size of α-U phase was large, with the modal average being 24.6 μm in diameter and exhibited a preferent α(101) orientation. It can observed that the surface of the "splat" would be subjected to the most rapid cooling, it is also the region where the γ-U is most likely to be preserved.

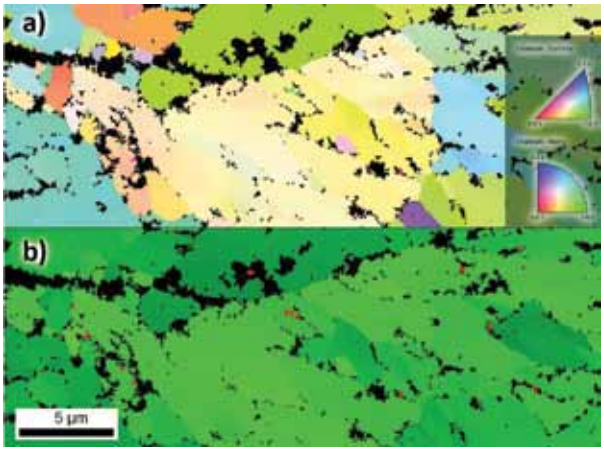

Fig. 5. EBSD maps for the pure uranium splat surface: a) crystallographic orientation and b) phase distribution. It is dominant α-U-phase (green colour) with small and well dispersed γ-U (red colour) grains [11]

EBSD maps illustrated the crystallographic and phase distribution for U-15 at.% Mo are shown in Fig. 6, exhibiting an equigranular grain structure, without crystal twinning and preferred crystallographic orientation. The results clearly indicated the presence of the cubic γ-U structure with no detectable orthorhombic α-U phase, providing a strong confirmation of the XRD results.

In the case of U-15 at.% Nb splat, EDX analysis showed a homogeneous distribution of Nb. Fig. 7 demonstrates the EBSD mapping of the crystallographic orientation and the phase distribution. The grains are colour-coded with respect to the inverse pole figure plot (shown in the insert) to represent their relative crystallographic orientation. EBSD mapping identified only the γ-U type phase. We notice here that XRD investigation indicates the existence of a γ°-U phase. Our equipment cannot resolve such a small structure deviation like the small tetragonal distortion of the γ-U structure (γ°-U phase). That is why the structure was identified as a normal γ-U structure. A small amount of the α-U phase (7%) was found, which is located at the γ-grain boundaries, but not forming a contiguous network. For some part of area the structure could not be identified, which is mostly likely due to fast forming oxidic overlayer [21].

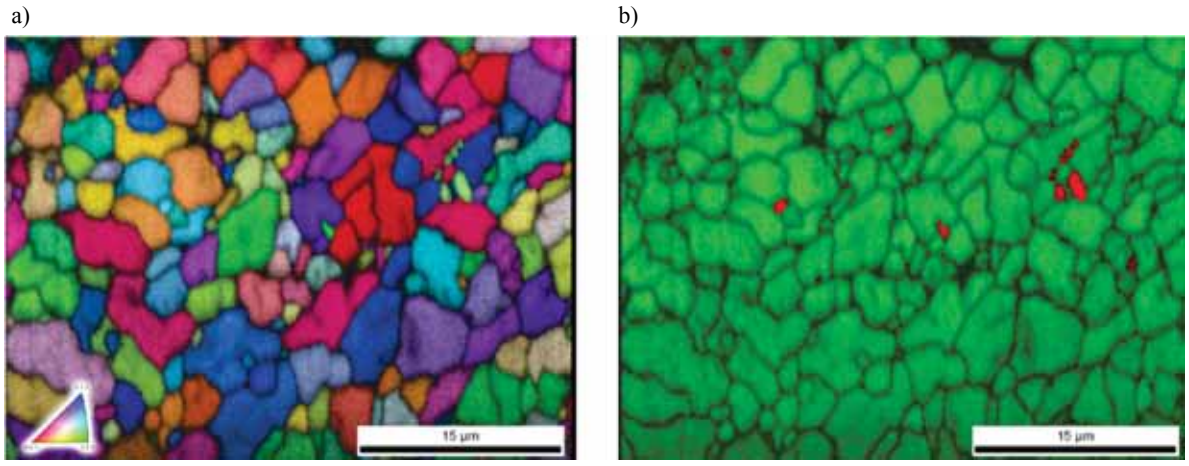

Fig. 6. EBSD crystallographic orientation (a) and phase distribution (b) of the splat-cooled U-15 at.% Mo alloy. EBSD mapping identified only γ-U phase, without a trace of α-U or α-related phases

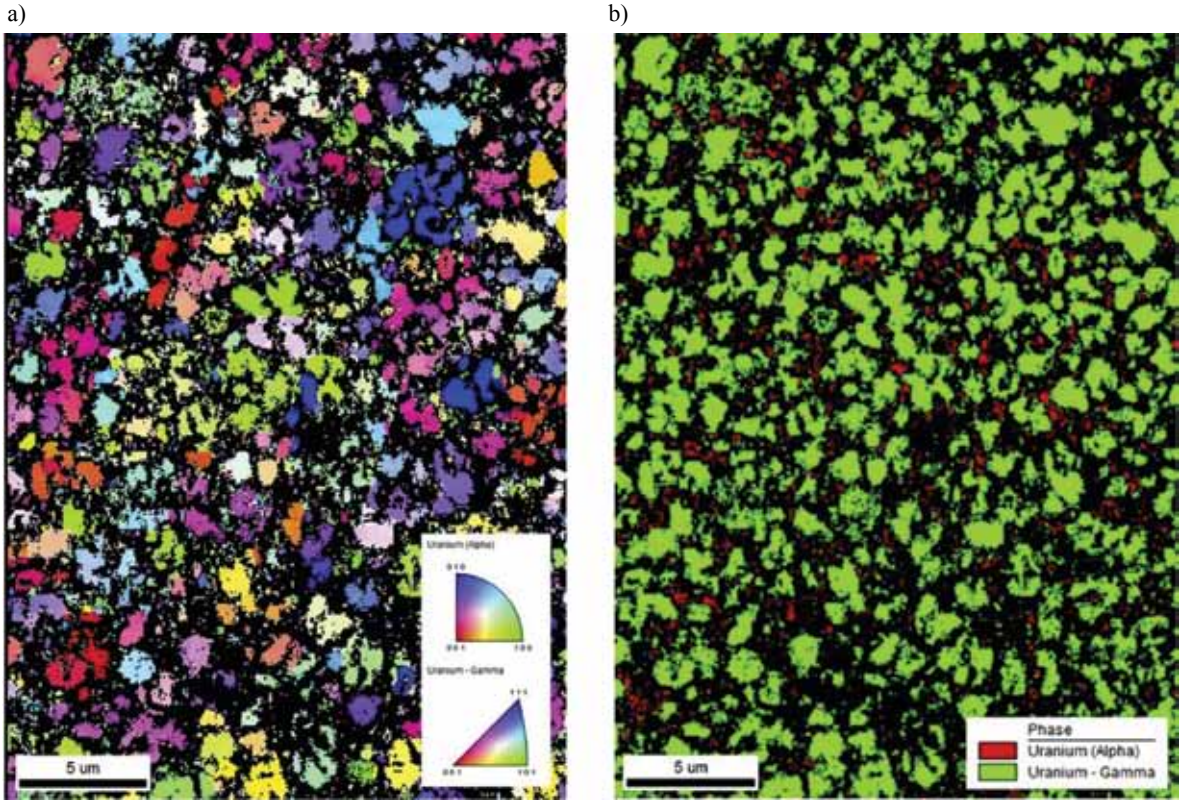

Fig. 7. EBSD crystallographic orientation (a) and phase distribution (b) of the splat-cooled U-15 at.% Nb alloy. The green colour represent γ-U phase and the red colour represent α-U phase. The black-coloured area is attributed to the oxidic overlayer [21]

The microstructure analysis was also performed for U-15 at.% Pt. Despite using the standard surface preparation, we could not get a surface that which would give reliable electron backscatter diffraction signals. We could only obtain the backscattered diffractions (BSD) images shown in Fig. 8. The results indicate that the material consists mainly of a single-phase with a bimodal structure with a grain size of 1–5 µm. The grey colour presents the phase in the interior of the grains which corresponds to the nominal stoichiometry (15 at.% Pt). Analysing the volume, which includes the grain-boundary area, the average Pt concentration is estimated to be around 26 at.%. The results suggest that the grain boundaries trend to be enriched by Pt. The white islands and dendrites of a size in the range of the 20–100 nm are certainly U-poor ones (rich Pt). The uranium oxides and oxynitrides were identified by areas of a black-colour [19].

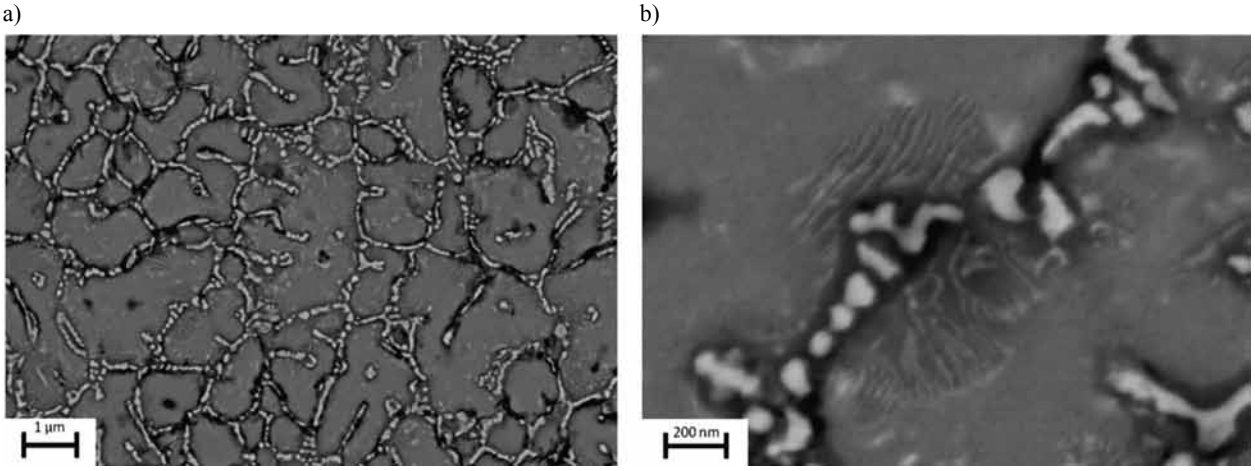

Fig. 8. The BSD images of U-15 at.% Pt splat for a large area (a) and its details (b). The main (grey-coloured) phase in the interior of the grains represent the nominal stoichiometry (of 15 at.% Pt) [19]

Conclusions

We have stabilized the cubic γ-U phase in U-T alloys by a combination of ultrafast cooling and alloying with ≥15 at.% T content (T = Mo, Nb, Pt, Ru and Ti). It is crucial that using the ultrafast cooling with a cooling rate 10^6 K/s we are able to reduce the necessary concentration of the T elements. In other words, the γ-U phase can be stabilized by a lower concentration of alloying elements by using splat cooling techniques. Alloying with 11–12 at.% Mo stabilizes the °-U phase (the tetragonally distorted variant of the cubic γ-U structure). U-15 at.% Mo splat-cooled alloy consists of an ideal cubic A2 structure. For the U-Ru system the pure cubic structure of the γ-U phase appeared for 12–15 at.% Ru. Thus, not only Mo but also Ru is sufficient for the stabilization of the pure cubic γ-U structure. Moreover, ultrafast cooling could also extend the solubility of Pt in U (up to at least 15 at.%). Therefore we can also stabilize the γ-U phase by alloying with 15 at.% Pt. However, the orthorhombic α-U phase is still present in this case. The pure cubic γ-U phase is also obtained in U-Nb and U-Ti alloys but with higher concentration (20 at.% Nb and U-30 at.% Ti).

EBSD results indicate that the pure (ideal) γ-U phase was stabilized in the whole sample of U-15 at.% Mo splat-cooled alloy.

Acknowledgements

We highly acknowledge the fruitful help with experiments of I. Tkach and M. Paukov.

References

1. Van Den Berghe S., Leenaers A., Koonen E., Sannen L.: From High to Low Enriched Uranium Fuel in Research Reactors. *Advances in Science and Technology,* 2010*,* 73, pp. 78–90.
2. Van Den Berghe S., Lemoine P.: Review of 15 years of High-Density Low-Enriched U-Mo Dispersion Fuel Development For Research Reactors in Europe. *Nuclear Engineering and Technology*, 2014, 46(2), pp. 125–146.
3. Sinha V.P., Hegde P.V., Prasad G.J., Dey G.K., Kamath H.S.*:* Phase transformation of metastable cubic γ-U phase in U-Mo alloys*. Journal of Alloys and Compounds,* 2010, 506(1), pp. 253–262.
4. Ewh A., Perez E., Keiser D., Jr D., Sohn Y.H.: Microstructural Characterization of U-Nb-Zr, U-Mo-Nb and U-Mo-Ti Alloys via Electron Microscopy*. Journal of Phase Equilibria and Diffusion*, 2010, 31(3), pp. 216–222.
5. Grenthe I., Drożdżyński J., Fujino T., Buck E.C., Albrecht-Schmitt T.E., Wolf S.F.: *Uranium*. In: Morss L.R., Edelstein N.M., J. Fuger J. (Eds): *The Chemistry of the Actinide and Transactinide Elements*. Netherlands, Dordrecht: Springer, 2006, pp. 253–698.
6. Yakel H.L.: A review of X-ray diffraction studies in uranium alloys. In: *Proceedings of the Physical Metallurgy of Uranium Alloys Conference*, *Vail, Colorado, USA, 1974*. [Online]. AEC Army Material and Mechanical Research Center, 1974. [Accessed 12 March 2019]. Available from: www.osti.gov/servlets/purl/4306144
7. Chiotti P., Klepfer H.H., White R.W.: Lattice parameters of uranium from 25 to 1132°C. *Transactions of American Society for Metals*, 1959, 51, pp. 772–782.
8. Lander L.H., Fisher E.S., Bader S.D.: The solid-state properties of uranium A historical perspective and review. *Advances in Physics,* 1994*,* 43 (1), pp. 1–111.
9. Lashley J.C., Lang B.E., Boerio-Goates J., Woodfield B.F., Schmiedeshoff G.M., Gay E.C.,

McPheeters C.C., Thoma D.J., Hults W.L., Cooley J.C., Hanrahan R.J., Smith J.L.: Low-temperature specific heat and critical magnetic field of α-uranium single crystal. *Physical Review B*, 2001, 63(224510), pp. 1–7.
10. Graf D., Stillwell R., Murphy T.P., Park J.-H., Kano M., Palm E.C., Schlottmann P., Bourg J., Collar K.N., Cooley J., Lashley J., Willit J., Tozer S.W.: Fermi surface of α-uranium at ambient pressure. *Physical Review B,* 2009*,* 80, 241101.
11. Tkach I., Kim-Ngan N.-T.H., Maskova S., Dzevenko M., Havela L., Warren A.D., Havela L., Sitt C., Scott T.B.: Characterization of cubic γ-phase uranium molybdenum alloys synthesized by ultrafast cooling, *Journal of Alloys and Compounds,* 2012*,* 534, pp.101–109.
12. Kim-Ngan N.-T.H., Tkach I., Maskova S., Goncalves A.P., Havela L.: Study of decomposition and stabilization of splat-cooled cubic -U phase U-Mo alloys. *Journal Alloys and Comp*ounds, 2013, 580, pp. 223–231.
13. Kim-Ngan N.-T.H., Paukov M., Sowa S., Krupska M., Tkach I., Havela L.: Structure and superconducting transition in splat-cooled U-T alloys. *Journal* of *Alloys and Compounds,* 2015*,* 645, pp. 158–163.
14. Krupska M., Kim-Ngan N.-T.H., Sowa S., Paukov M., Tkach I., Drozdenko D., Havela L., Tarnawski Z.: Structure, Electrical Resistivity and Superconductivity of Low-alloyed γ-U Phase Retained to Low Temperatures by Means of Rapid Cooling. *Acta Metalurgica Sinica (English Letter),* 2016, 29(4), pp. 388–398.
15. Hills R.F.,Howlett B.W., Butcher B.R.: Further studies on the decomposition of the γ phase in uranium-low molybdenum alloys*. Journal of Less Common Metals,* 1963, 5(5), pp. 369–373.
16. Lehmann J., Hills R.F.: Proposed nomenclature for phases in uranium alloys. *Journal of Nuclear Materials*, 1960, 2(3), pp. 261–268.
17. Hills R.F., Howlett B.W., Butcher B.R., Steward D.: The effect of cooling rate on the decomposition of the γ-phase in uranium-zirconium alloys. *Journal of Nuclear Materials,* 1965, 16(1), pp.109–128.
18. Sowa S., Kim-Ngan N.-T.H., Krupska M., Paukov M., Buturlim V., Havela L.: Structure and properties of U alloys with selected d-metals and their hydrides. *Physica B: Condensed Matter*, 2018, 536, pp. 546–552.
19. Kim-Ngan N.-T.H., Havela L., Paukov M., Drozdenko D., Minarik P., Chrobak M., Tarnawski Z., Sowa S., Krupska M., Duda A.: Superconductivity in U-Pt system with low Pt concentrations (≤15at.%). *Physica C: Superconductivity and its Applications,* 2018*,* 546, pp. 76–83.
20. Kim-Ngan N.-T.H., Tarnawski Z., Chrobak M., Sowa S., Duda A., Paukov M., Buturlim V., Havela L.: Superconducting phase transitions in mK temperature range in splat-cooled $U_{0.85}Pt_{0.15}$alloys. *Physica B: Condensed Matter*, 2018, 536, pp. 708––712.
21. Kim-Ngan N.-T.H., Sowa S., Krupska M., Paukov M., Drozdenko D., Minarik P., Havela L.: Superconductivity in U-Nb alloys with γ-U phase and ferromagnetism of their hydrides. *Physica B: Condensed Matter,* 2018, 545, pp. 152–158.